



Investigation on the Linear Energy Storage and Dissipation Laws of Rock Materials Under Uniaxial Compression

Fengqiang Gong^{1,2} · Jingyi Yan¹ · Song Luo¹ · Xibing Li^{1,2}

Received: 10 July 2018 / Accepted: 1 May 2019 / Published online: 21 May 2019
© Springer-Verlag GmbH Austria, part of Springer Nature 2019

Abstract

To investigate the energy evolution characteristics of rock materials under uniaxial compression, the single-cyclic loading–unloading uniaxial compression tests of four rock materials (Qingshan granite, Yellow sandstone, Longdong limestone and Black sandstone) were conducted under five unloading stress levels. The stress–strain curves and failure characteristics of rock specimens under the single-cyclic loading–unloading uniaxial compression tests basically corresponded with those of under uniaxial compression, which indicates that single-cyclic loading–unloading has minimal effects on the variations in the loading–deformation response of rocks. The input energy density, elastic energy density and dissipated energy density of four rocks under five unloading stress levels were calculated using the graphical integration method, and variation characteristics of those three energy density parameters with different unloading stress levels were explored. The results show that all three energy density parameters above increased nonlinearly with increasing unloading stress level as quadratic polynomial functions. Meanwhile, both the elastic and dissipated energy density increased linearly when the input energy density increased, and the linear energy storage and dissipation laws for rock materials were observed. Furthermore, a linear relationship between the dissipated and elastic energy density was also proposed. Using the linear energy storage or dissipation law, the elastic and dissipated energy density at any stress levels can be calculated, and the internal elastic (or dissipated) energy density at peak compressive strength (the peak elastic and dissipated energy density for short) can be obtained. The ratio of the elastic energy density to dissipated energy density with increasing input energy density was investigated using a new method, and the results show that this ratio tends to be constant at the peak compressive strength of rock specimens.

Keywords Rock materials · Input energy density · Elastic energy density · Linear energy storage law · Linear energy dissipation law · Peak elastic energy density · Single-cyclic loading–unloading uniaxial compression

List of Symbols

D	Diameter of specimen	u^e	Elastic energy density of rock at peak compressive strength (the peak elastic energy density for short)
E_u	Linear modulus of ideal unloading curve at peak strength	u^d	Dissipated energy density of rock at peak compressive strength (the peak dissipated energy density for short)
E_s	Unloading tangential modulus	u^o	Input energy density of rock at peak compressive strength (the peak input energy density for short)
E_1	Loading curve's Young's modulus	u_i^d	Dissipated energy density at actual unloading stress level i
H	Height of specimen	u_i^e	Elastic energy density at actual unloading stress level i
i	Actual unloading stress level	u_d^o	Input energy density at any loading time before the peak compressive strength
k	Setting unloading stress level	u_i^o	Input energy density at actual unloading stress level i
		u_i^d/u_i^o	Ratio of the dissipated energy density to the input energy density

✉ Fengqiang Gong
fengqiangg@126.com

¹ School of Resources and Safety Engineering, Central South University, Changsha 410083, Hunan, China

² Hunan Key Laboratory of Resources Exploitation and Hazard Control for Deep Metal Mines, Changsha 410083, Hunan, China

u_i^e/u_i^o	Ratio of the elastic energy density to the input energy density
v	Longitudinal wave speed of the specimen
V	Volume of specimen
W_{et}^d	Ratio of the elastic energy density to the dissipated energy density when the input energy density is u_d^o
W_{et}^i	Ratio of the elastic energy density to the dissipated energy density at actual unloading stress level i and is equal to u_i^e/u_i^d
W_{et}^p	Ratio of the peak elastic energy density to the peak dissipated energy density and is equal to u^e/u^d

Greek Symbols

ρ	Density of specimen
σ_c^e	Uniaxial compressive strength of specimen
σ_c^k	Peak compressive strength of specimen under single-cyclic loading–unloading uniaxial compression when setting unloading stress level is k

Abbreviations

DED	Dissipated energy density
EED	Elastic energy density
IED	Input energy density
SCLUC	Single-cyclic loading–unloading uniaxial compression
UC	Uniaxial compression

1 Introduction

The process of rock fracture and failure is essentially an energy transfer and exchange event, and the energy-related characteristics are important and effective in describing the mechanical properties of rock materials. The rock deformation and failure process is intrinsically driven by energy evolution activities that include energy input, storage, dissipation and release (Brady and Brown 2006; Xie et al. 2005; Mcsaveney and Davies 2009; Wasantha et al. 2014; Park et al. 2014; Wang et al. 2017; Gong et al. 2018a). Many researchers have conducted experimental studies from different aspects to investigate the energy evolution characteristics of rock materials. Based on uniaxial compression (UC) tests, Tsoutrelies and Exadaktylos (1993) studied the effects of rock discontinuities on the ratio of surface energy to the volume elastic strain energy. Hua and You (2001) concluded that the strain energy is stored in rocks during the loading stage, and the energy will be released when it is sufficiently large, causing rock failure. Huang and Li (2014) investigated the characteristics of strain energy accumulation, dissipation and release in three stages, including elastic compression, pre-peak unloading and post-peak fracturing. Li et al. (2014) analyzed the strain rate dependency of rock strain energy

and observed that the pre-peak absorbs strain energy, while damage strain energy and elastic strain energy increase with the strain rate. Meng et al. (2016, 2018) revealed the acoustic emission characteristics of rocks and identified the relationships between the elastic energy, dissipated energy and axial loading stress of rock specimens. Xu and Cai (2018) investigated the influence of the strain energy released from a UC test machine on the rock failure process. Gong et al. (2018b, c) studied the energy storage and dissipation evolution process and characteristics of red sandstone and marble in three tension-type failure tests (including Brazilian test, point load test and semi-circular bending test), and found that there are linear relationships between the internal elastic and dissipated and external input energy. On the other hand, triaxial compression tests have also been performed to investigate energy transformation during deformation and failure process of rock. Peng et al. (2015) obtained the relationship between energy transformation and coal failure with conventional triaxial compression tests under five different confining pressures. Yang et al. (2016) proposed energy dissipation and energy release rules to characterize crack growth under different triaxial stress and explained the relationships between the releasable elastic strain energy, the dissipated energy density and the confining pressure. Zhang et al. (2017) explored the influence of confining pressure on the energy evolution characteristics and distribution relationships through triaxial cyclic loading–unloading compression tests. Torabi and Zarifi (2014) investigated the energy propagation in rock cataclastic bands. Castanon-Jano et al. (2017) designed energy dissipating devices from the perspective of energy conversion. Li et al. (2019) studied the energy attenuation characteristics of rock masses with different joint roughness using the modified SHPB device. Furthermore, certain rockburst proneness indexes were also proposed based on energy analysis (Kidybinski 1981; Singh 1988; Wang and Park 2001). Jiang et al. (2010) and Li et al. (2012) used a new energy index LERR (local energy release rate) to simulate and analyze the conditions causing rockburst in the deeply buried tunnels of Jinping II hydropower station. Cai (2016) and Miao et al. (2016) analyzed rockburst disasters in rock engineering from the prospect of energy accumulation theory. Gong et al. (2019) proposed a peak strength strain energy storage index to estimate and classify the rockburst proneness of nine rock materials.

According to the existing literature studies, most of the relevant research studies focus on the relationships between the elastic energy (or dissipated energy) and the stress or strain of rock specimen during the loading process. Few studies have emphasized the relationships between the input energy density (IED), elastic energy density (EED) and dissipated energy density (DED). In the present study, four rock materials (Qingshan granite, Yellow sandstone, Longdong limestone and Black sandstone) were investigated

by single-cyclic loading–unloading uniaxial compression (SCLUC) tests under five unloading stress levels. The conversion characteristics of three energy density parameters (IED, EED and DED) with unloading stress levels were studied. Additionally, the relationships among the EED, DED and IED were analyzed in detail. The results show that there are strong linear relationships between the EED, DED and IED for every rock type tested. Based on the linear energy storage law, the EED or DED can be calculated at any stress levels. The proportional relationships between the EED and DED with increasing IED were also discussed.

2 Experimental Study

2.1 Rock Specimens and Preparation

A series of tests were carried out on four rock materials taken from different quarry in China; Qingshan granite and Longdong limestone materials were obtained from the city of Changsha in the Hunan Province, and Yellow sandstone and Black sandstone were taken from the city of Zigong in the Sichuan province. All the rock materials had favorable integrities and compactness without surface cracks. Cylindrical specimens were obtained by drilling core. The diameter (D) of the rock specimens was 50 mm, and the height (H) was 100 mm. The sides and end faces of the rock specimens were smoothed before testing. The nonparallel end faces and axial deviation were in the allowable ranges according to the standards of the International Society for Rock Mechanics (ISRM) standard (Fairhurst and Hudson 1999). Six specimens of each rock material with good homogeneity were selected for testing, and photographs of these specimens are shown in Fig. 1. The basic parameters of each rock specimen were determined, and the results are presented in Table 1. The density (ρ) of the Qingshan granite, Yellow sandstone, Longdong limestone and Black sandstone varied from 2.63 to 2.66 g/cm³, 2.57 to 2.58 g/cm³, 2.68 to 2.70 g/cm³ and 2.58 to 2.60 g/cm³, respectively. The longitudinal wave velocities (v) ranges were 3937.60–4248.83 m/s,

3872.17–4036.47 m/s, 6096.66–6193.23 m/s and 3645.34–3792.08 m/s, respectively.

2.2 Test Instrument and Test Schemes

The tests on the four rocks were all carried out with INSTRON 1346 testing system (Fig. 2). The testing system includes a control computer, loading system, pressure chambers, hydraulic transmission system and data acquisition system. During the tests, the axial forces of the rock specimens were obtained through the pressure sensor of the testing machine. The axial displacement of rock specimens was measured by linear variable differential transformers (LVDTs). First, the uniaxial compressive strength (σ_c^e) of a rock specimen was obtained by UC test and was taken as the initial estimated peak compressive strength. Second, the setting unloading stress level ($k = 0.1, 0.3, 0.5, 0.7, 0.9$) of unloading point was determined in accordance with the σ_c^e of rocks, and thus, the unloading stress $k\sigma_c^e$ was obtained. Then, SCLUC tests under different setting unloading stress levels were performed, and the peak compressive strength σ_c^k of every specimen was obtained. After obtaining the σ_c^k , the actual unloading stress level i of every specimen was calculated as follows:

$$i = k\sigma_c^e / \sigma_c^k. \quad (1)$$

The stress–strain curves of the rock specimens under SCLUC paths are shown in Fig. 3. The entire loading process was divided into three stages, namely initial loading stage, unloading stage and secondary loading stage.

3 Stress–Strain Curves and Failure Characteristics of Rock Specimens

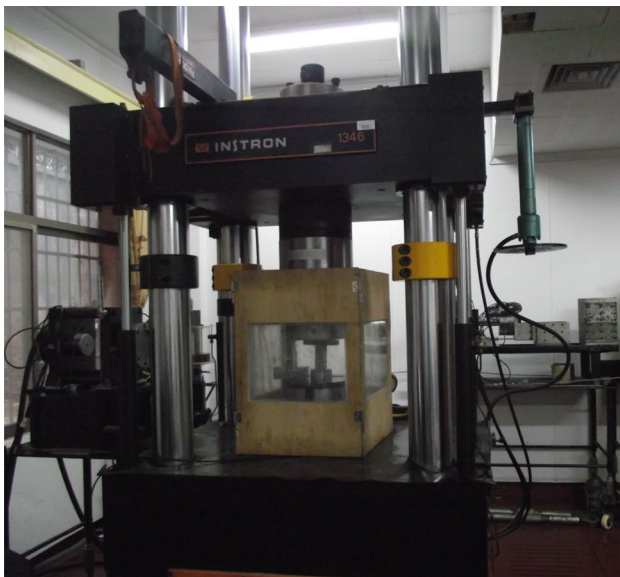
The stress–strain curves of four rock materials under the UC and SCLUC tests are presented in Figs. 4 and 5. The specific parameters of each rock specimen are shown in Table 2. It can be observed that the peak compressive strength of different specimens for each rock material is very similar. The

Fig. 1 Photographs of rock specimens (left to right): Qingshan granite, Yellow sandstone, Longdong limestone, Black sandstone (color figure online)

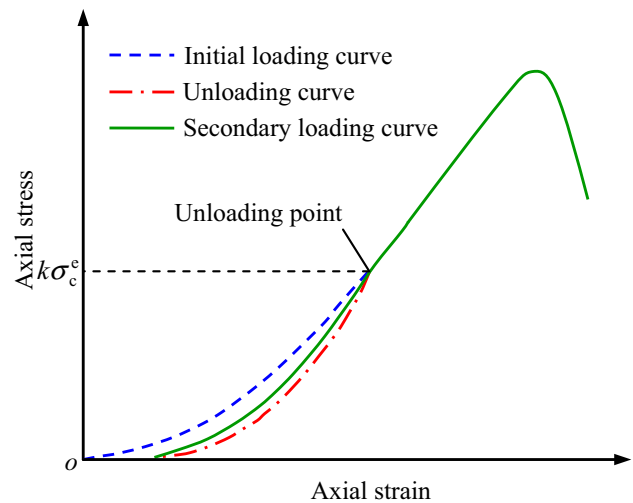


Table 1 Basic parameter of rock specimens

Rock type	Specimen no.	D (mm)	H (mm)	V (cm ³)	v (m/s)	ρ (g/cm ³)
Qingshan granite	QM-1	48.68	100.25	186.49	4168.40	2.64
	QC-1	49.40	101.59	194.61	3937.60	2.64
	QC-2	49.37	100.61	192.50	3953.24	2.63
	QC-3	48.78	100.37	187.48	4217.23	2.64
	QC-4	48.78	100.06	186.90	4248.83	2.66
	QC-5	49.43	101.18	194.06	3967.84	2.63
Yellow sandstone	YM-1	48.57	101.10	187.22	3918.60	2.57
	YC-1	48.58	100.85	186.84	3986.17	2.57
	YC-2	48.58	100.87	186.87	3872.17	2.57
	YC-3	48.66	101.35	188.38	3974.51	2.57
	YC-4	48.59	100.98	187.15	3983.43	2.58
	YC-5	48.60	100.71	186.73	4036.47	2.58
Longdong limestone	LM-1	48.62	100.64	186.75	6193.23	2.68
	LC-1	48.61	100.99	187.33	6139.21	2.70
	LC-2	48.75	100.42	187.34	6123.17	2.68
	LC-3	48.59	100.93	187.06	6154.27	2.69
	LC-4	48.62	100.28	186.09	6114.63	2.69
	LC-5	48.67	100.29	186.49	6096.66	2.69
Black sandstone	BM-1	48.64	100.46	186.57	3790.94	2.60
	BC-1	48.64	100.49	186.63	3792.08	2.58
	BC-2	48.64	100.43	186.52	3678.75	2.59
	BC-3	48.64	100.79	187.19	3746.84	2.59
	BC-4	48.64	99.70	185.16	3645.34	2.60
	BC-5	48.64	100.37	186.41	3752.15	2.58

**Fig. 2** INSTRON 1346 testing machine

secondary loading curves will intersect the unloading curve at a stress slightly smaller than $k\sigma_c^e$ and continue to develop along the development trend of the initial loading line, which demonstrates that rock material possesses a memory

**Fig. 3** Stress–strain curve of rock specimen under SCLUC path

function and the SCLUC process has little effect on the variation trend of stress–strain curves. Figure 5 also shows that the strain of the unloading curve will not reach zero point when the unloading stress is zero. There is an obvious area between the initial loading curve and unloading curve, which represents energy that was dissipated (Jaeger et al.; 2007).

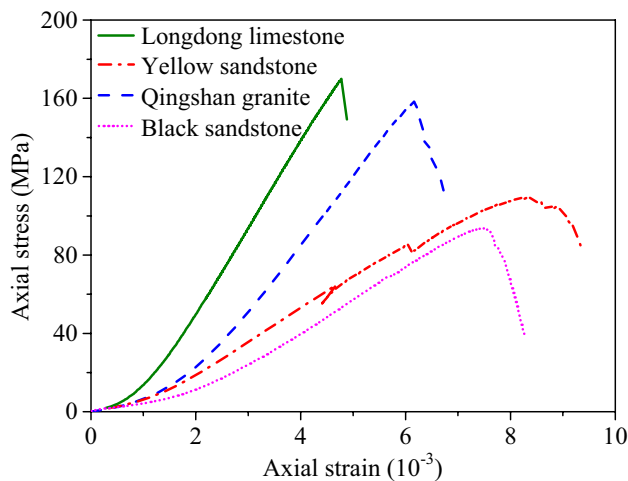


Fig. 4 Stress–strain curves of rock specimens in the UC test

The failure characteristics of the rock specimens under UC are shown in Fig. 6. Figure 6a, b, d shows that failure modes of Qingshan granite, Yellow sandstone and Black sandstone specimens are all shear failure. In Fig. 6c, the Longdong limestone specimens mainly fail by splitting. All the failures occurred instantaneously, while the crack initiation and propagation in the failure process were unapparent. Regardless of whether the specimens were under UC or SCLUC, the failure modes of specimens for each rock material were the same, which indicates that the SCLUC has no effect on the failure characteristics.

4 Energy Conversion Characteristics During Loading Process

4.1 Energy Calculation Method of Three Energy Parameters

Based on the energy equation of rocks during loading process proposed by Xie et al. (2009), the equivalent relationship among three energy parameters of rock specimens under the actual unloading stress level i can be expressed as

$$u_i^o = u_i^e + u_i^d, \quad (2)$$

where u_i^o is the IED at the actual unloading stress level i , u_i^e is the EED at the actual unloading stress level i , and u_i^d is the DED at the actual unloading stress level i . Furthermore, the relationship among the peak IED (u^o), peak EED (u^e) and peak DED (u^d) can also be expressed as

$$u^o = u^e + u^d. \quad (3)$$

The product of the IED and the volume of a rock specimen is equivalent to the total work performed by the testing machine on the specimen. The product of the EED and

volume of a rock specimen is the elastic energy stored in rock, which can be regenerated during the unloading process. The dissipated energy is equivalent to the product of the DED and volume of rock specimen, which is used for crack propagation, rock plastic deformation, thermal energy, acoustic emission energy and so on (Song et al. 2012; Ai et al. 2016).

The IED, EED and DED can be obtained by integrating the enclosed area. The integration area of different energy density parameters is shown in Fig. 7. Under different unloading stress levels, the IED of a rock specimen is estimated as the area enclosed by the initial loading stress–strain curve and the abscissa axis. The EED is calculated by the area under the unloading stress–strain curve and the abscissa axis, and the enclosed area of the initial loading and unloading curve is DED (Kidybiński 1981; Zhang and Gao 2015).

4.2 Energy Evolution of Rock Specimens Under Different Actual Unloading Stress Levels

Using the calculation method mentioned in Sect. 4.1, the IED, EED and DED of rock specimens under different actual unloading stress levels were obtained (see Table 3).

Figure 8 shows the change rule of IED, EED and DED with the actual unloading stress level. To improve the fitting accuracy, an extra (0, 0) point was added in each figure. As given by Fig. 8, the IED, EED and DED of the four rock materials all present nonlinear growth with increasing unloading stress level. The IED grows the most rapidly of the three energy densities, followed by the EED and then DED. The curve of the EED is closer to the IED, which indicates that a larger amount of the external input energy is transformed into the elastic energy, and the dissipated energy only occupies a small part of the input energy. In addition, it can be seen from Fig. 8 that the higher the compressive strength of the rock (the average compressive strengths of Qingshan granite, Yellow sandstone, Longdong limestone and Black sandstone are 156.64, 117.62, 161.53 and 87.16 MPa, respectively), the closer the EED is to the IED. This result indicates that a higher compressive strength usually represents a stronger energy storage capacity and more obvious elastic brittleness in rock, which corresponds the general understanding of the energy storage characteristics of rock materials. These characteristics are also confirmed in Figs. 4 and 5. The post-peak curves of Longdong limestone are relatively short, while those of Yellow sandstone and Black sandstone are relatively long.

To further assess the relationships between the IED, EED and DED and the actual unloading stress level, a quadratic polynomial function was used to fit the variation laws. The nonlinear relationships between u_i^o , u_i^e , u_i^d and i of Qingshan granite, Yellow sandstone, Longdong limestone and Black sandstone are shown in Table 4. It can

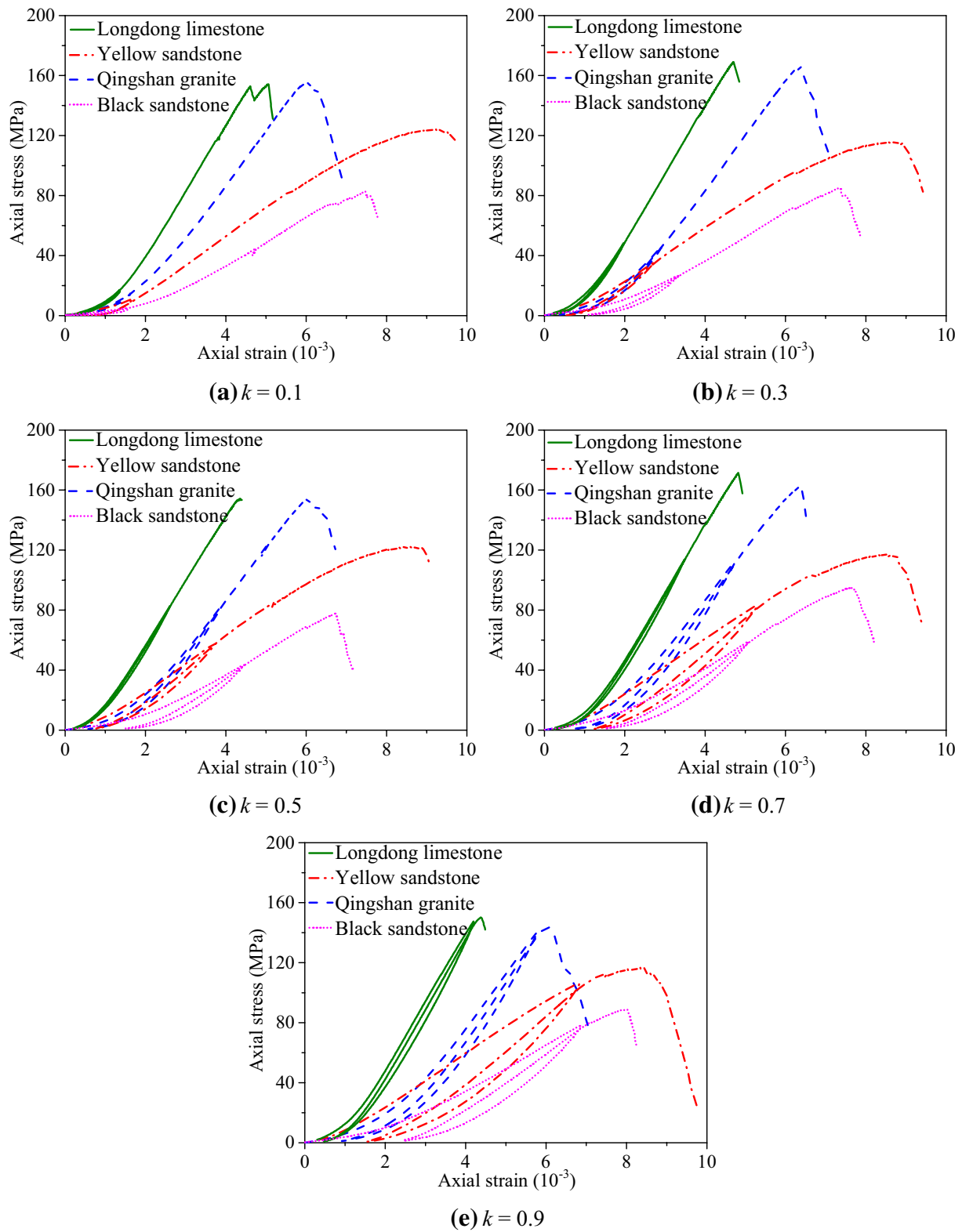


Fig. 5 Stress–strain curves of rock specimens in SCLUC test under different unloading stress level k

Table 2 Parameters of rock specimens at different unloading points

Rock type	Specimen no.	Test type	Unloading point			Peak compressive strength (MPa)
			Setting unloading stress level (k)	Stress value (MPa)	Actual unloading stress level (i)	
Qingshan granite	QM-1	UC	–	–	–	158.66
	QC-1	SCLUC	0.10	15.50	0.0998	155.35
	QC-2		0.30	48.87	0.2952	165.56
	QC-3		0.50	81.47	0.5269	154.61
	QC-4		0.70	112.45	0.6936	162.14
	QC-5		0.90	141.18	0.9835	143.55
Yellow sandstone	YM-1	UC	–	–	–	109.33
	YC-1	SCLUC	0.10	11.18	0.0898	124.39
	YC-2		0.30	35.26	0.3046	115.75
	YC-3		0.50	58.18	0.4756	122.32
	YC-4		0.70	83.05	0.7090	117.14
	YC-5		0.90	106.26	0.9100	116.76
Longdong limestone	LM-1	UC	–	–	–	169.91
	LC-1	SCLUC	0.10	17.04	0.1105	154.20
	LC-2		0.30	48.48	0.2868	169.04
	LC-3		0.50	82.70	0.5361	154.27
	LC-4		0.70	113.83	0.6638	171.49
	LC-5		0.90	147.47	0.9814	150.26
Black sandstone	BM-1	UC	–	–	–	93.70
	BC-1	SCLUC	0.10	4.94	0.0597	82.71
	BC-2		0.30	26.47	0.3107	85.20
	BC-3		0.50	43.45	0.5587	77.77
	BC-4		0.70	59.17	0.6231	94.95
	BC-5		0.90	77.91	0.8791	88.63

be seen from Table 4 that the coefficient correlation R^2 of the fitting functions is all greater than 0.98. A quadratic polynomial function can describe the relationship between the three energy density parameters and actual unloading stress level well. Figure 9 shows the variation of the ratios u_i^e / u_i^o and u_i^d / u_i^o under different actual unloading stress levels. In Fig. 9a, c, the values of u_i^e / u_i^o are obviously higher than those of u_i^d / u_i^o , fluctuating around a constant value. These results also indicate that the input energy of Qingshan granite and Longdong limestone is mainly transformed into elastic energy. In Fig. 9b, d, when the unloading stress level is relatively low (less than 0.1–0.2), values of u_i^d / u_i^o are higher than those of u_i^e / u_i^o , indicating that energy consumption is the main factor. When the unloading stress level increases, the values of u_i^e / u_i^o become greater than those of u_i^d / u_i^o , and u_i^e / u_i^o first increases and then decreases. Furthermore, Fig. 9 also shows that when the unloading stress level increases (more than 0.2), the higher the compressive strength of rock, the larger the mean value of the gap between u_i^e / u_i^o and u_i^d / u_i^o , which indicates that the compressive strength of rock is positively correlated with its elastic energy storage capacity.

4.3 Relationships Among the IED, EED and DED

The relationships between the EED, DED and IED under different unloading stress levels were further investigated. Based on the data in Table 3, relationship curves are obtained in which the abscissa represents the IED, and the ordinate represents the EED and DED, respectively (shown in Fig. 10). Figure 10 shows that both u_i^e and u_i^d gradually increase with the increase of u_i^o , and there is an obvious linear correlation between u_i^e and u_i^d and u_i^o . The fitting functions can be expressed as follows:

$$u_i^e = au_i^o + b, \quad (4)$$

$$u_i^d = (1 - a)u_i^o - b, \quad (5)$$

where a and b are the fitting parameters obtained from experimental data. The fitting functions between u_i^e and u_i^d and u_i^o of the four rocks are presented in Table 5. The coefficients correlation R^2 of all the fitting functions range from 0.9377 to 0.9998, showing that there are strong linear relationships between them.



Fig. 6 Failure models of four rocks after UC and SCLUC tests

Taking Qingshan granite as an example, in Eq. (4), the slope a and intercept b are equal to 0.8010 and 0.0010, respectively. The coefficient b is very small compared with a , being only 0.12% of a . When the u_i^o increases, the effect of b on the function relation can gradually be ignored, and the fitting function simplifies to the form of $u_i^c = au_i^o$ ($u_i^c = 0.8010u_i^o$). The coefficient a reflects the ability to convert the input energy into elastic energy. Furthermore, the relationship between u_i^d and u_i^o can

be similarly described. The fitting function between u_i^d and u_i^o can be approximated to $u_i^d = (1 - a)u_i^o$ ($u_i^d = 0.1990u_i^o$). The coefficient $(1 - a)$ reflects the proportion of dissipated energy in the input energy. The above analysis is also applicable to Yellow sandstone, Longdong limestone and Black sandstone. The two constants a and $(1 - a)$ can be regarded as the compression

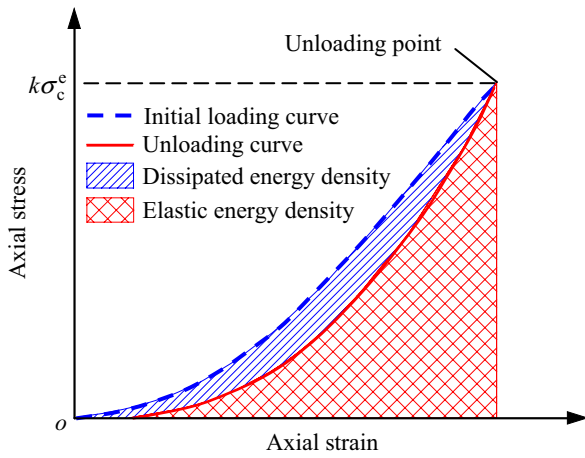


Fig. 7 Integration area of different energy density parameters

energy storage coefficient and the compression energy dissipation coefficient of rock materials separately.

Figure 11 shows the relationships between u_i^e and u_i^d , and the relationship is also a linear functional correlation as follows:

$$u_i^d = cu_i^e + d, \tag{6}$$

where c and d are fitting parameters obtained from experimental data. The R^2 of the linear function is all greater than

0.91 (shown in Table 5), showing that there is also a strong linear relationship between them. This function reflects the proportional relationship between the elastic energy and dissipated energy of rock specimen during loading process. In the case of achieving the EED, the DED can be obtained.

4.4 Application of the Linear Energy Storage or Dissipation Law

Using the obtained linear energy storage law, the EED or DED at any stress levels can be calculated for a rock material, especially at the peak strength of rock specimen. According to Eqs. (3)–(5) and u^o obtained from the stress–strain curve, u^e and u^d can be given as

$$u^e = au^o + b, \tag{7}$$

$$u^d = (1 - a)u^o - b, \tag{8}$$

Table 6 presents the u^o , u^e and u^d of the specimen in the UC and SCLUC tests. All the u^o s of the four rocks are compared in Fig. 12. The results show that all the u^o are random and that SCLUC operation produces a negligible effect compared with UC.

Table 3 Values of IED, EED and DED under the different actual unloading stress levels

Rock type	Specimen no.	Unloading stress level (i)	u_i^o (mJ/mm ³)	u_i^e (mJ/mm ³)	u_i^d (mJ/mm ³)	u_i^e/u_i^o	u_i^d/u_i^o	u_i^e/u_i^d
Qingshan granite	QC-1	0.0998	0.0087	0.0074	0.0013	0.8506	0.1494	5.6923
	QC-2	0.2952	0.0463	0.0381	0.0082	0.8229	0.1771	4.6463
	QC-3	0.5269	0.1102	0.0919	0.0183	0.8339	0.1661	5.0219
	QC-4	0.6936	0.1967	0.1583	0.0384	0.8048	0.1952	4.1224
	QC-5	0.9835	0.2989	0.2397	0.0592	0.8019	0.1981	4.0490
Yellow sandstone	YC-1	0.0898	0.0075	0.0034	0.0041	0.4533	0.5467	0.8293
	YC-2	0.3046	0.0390	0.0272	0.0118	0.6974	0.3026	2.3051
	YC-3	0.4756	0.0914	0.0659	0.0255	0.7210	0.2790	2.5843
	YC-4	0.7090	0.1966	0.1260	0.0706	0.6409	0.3591	1.7847
	YC-5	0.9100	0.3386	0.2007	0.1379	0.5927	0.4073	1.4554
Longdong limestone	LC-1	0.1105	0.0080	0.0067	0.0013	0.8375	0.1625	5.1538
	LC-2	0.2868	0.0343	0.0300	0.0043	0.8746	0.1254	6.9767
	LC-3	0.5361	0.0838	0.0776	0.0062	0.9260	0.0740	12.5161
	LC-4	0.6638	0.1510	0.1377	0.0133	0.9119	0.0881	10.3534
	LC-5	0.9814	0.2492	0.2150	0.0342	0.8628	0.1372	6.2865
Black sandstone	BC-1	0.0597	0.0038	0.0016	0.0022	0.4211	0.5789	0.7273
	BC-2	0.3107	0.0333	0.0192	0.0141	0.5766	0.4234	1.3617
	BC-3	0.5587	0.0724	0.0442	0.0282	0.6105	0.3895	1.5674
	BC-4	0.6231	0.1166	0.0737	0.0429	0.6321	0.3679	1.7179
	BC-5	0.8791	0.2101	0.1241	0.0860	0.5907	0.4093	1.4430

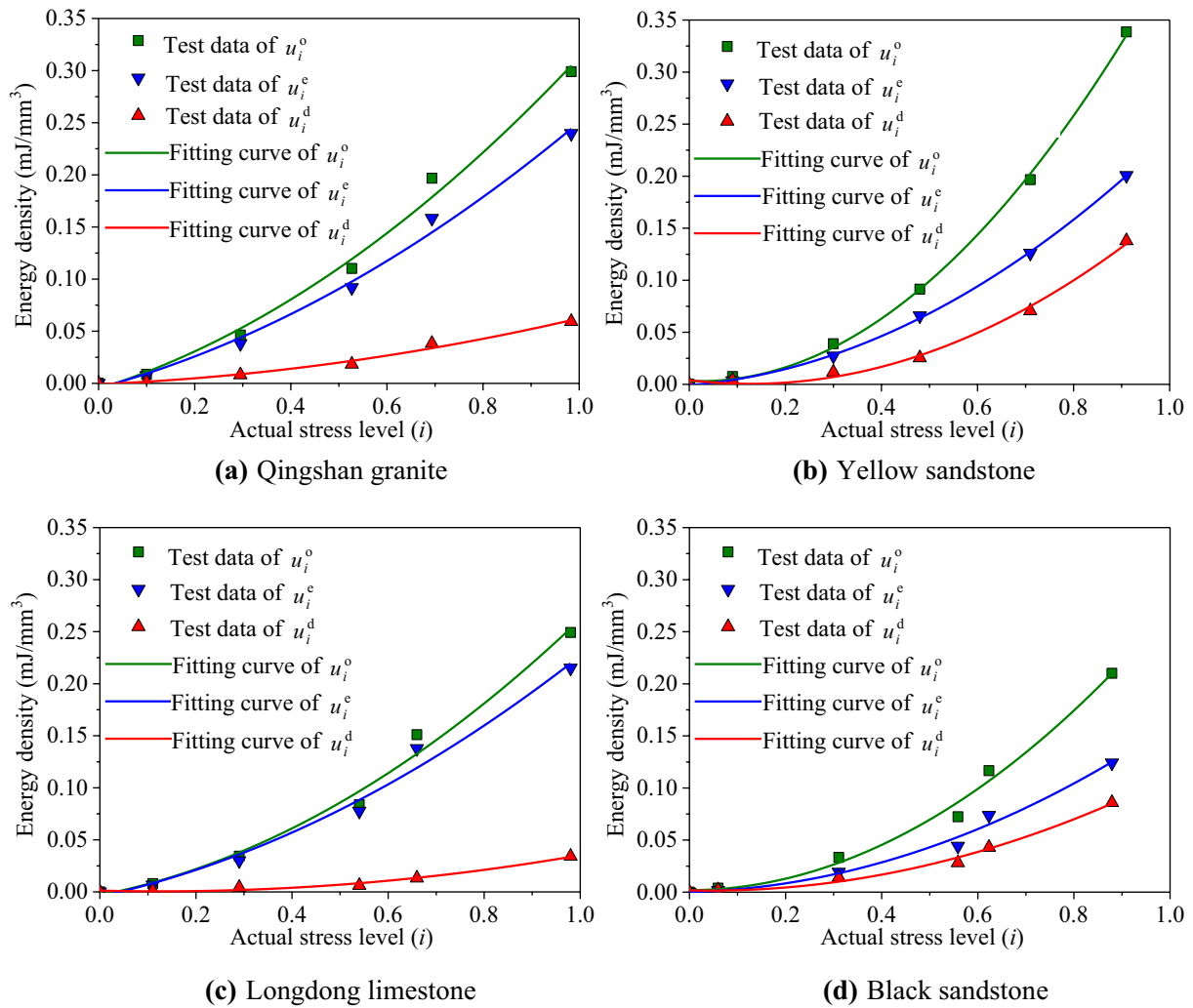


Fig. 8 The change laws of three energy density parameters with the actual stress level *i*

Table 4 Fitting functions and R^2 between u_i^o , u_i^e , u_i^d and *i*

Rock type	Fitting function for u_i^o and <i>i</i>	Fitting function for u_i^e and <i>i</i>	Fitting function for u_i^d and <i>i</i>
Qingshan granite	$u_i^o = 0.1730i^2 + 0.1451i - 0.0053$ ($R^2 = 0.9926$)	$u_i^e = 0.1296i^2 + 0.1254i - 0.0045$ ($R^2 = 0.9935$)	$u_i^d = 0.0434i^2 + 0.0198i - 0.0008$ ($R^2 = 0.9874$)
Yellow sandstone	$u_i^o = 0.4199i^2 - 0.0165i + 0.0030$ ($R^2 = 0.9993$)	$u_i^e = 0.2011i^2 + 0.0383i - 0.0009$ ($R^2 = 0.9994$)	$u_i^d = 0.2188i^2 - 0.0548i + 0.0039$ ($R^2 = 0.9948$)
Longdong limestone	$u_i^o = 0.1720i^2 + 0.0923i - 0.0032$ ($R^2 = 0.9900$)	$u_i^e = 0.1270i^2 + 0.1036i - 0.0045$ ($R^2 = 0.9866$)	$u_i^d = 0.0450i^2 - 0.0113i + 0.0013$ ($R^2 = 0.9842$)
Black sandstone	$u_i^o = 0.2672i^2 + 0.0019i + 0.0019$ ($R^2 = 0.9900$)	$u_i^e = 0.1481i^2 + 0.0117i + 0.0002$ ($R^2 = 0.9867$)	$u_i^d = 0.1191i^2 - 0.0099i + 0.0017$ ($R^2 = 0.9907$)

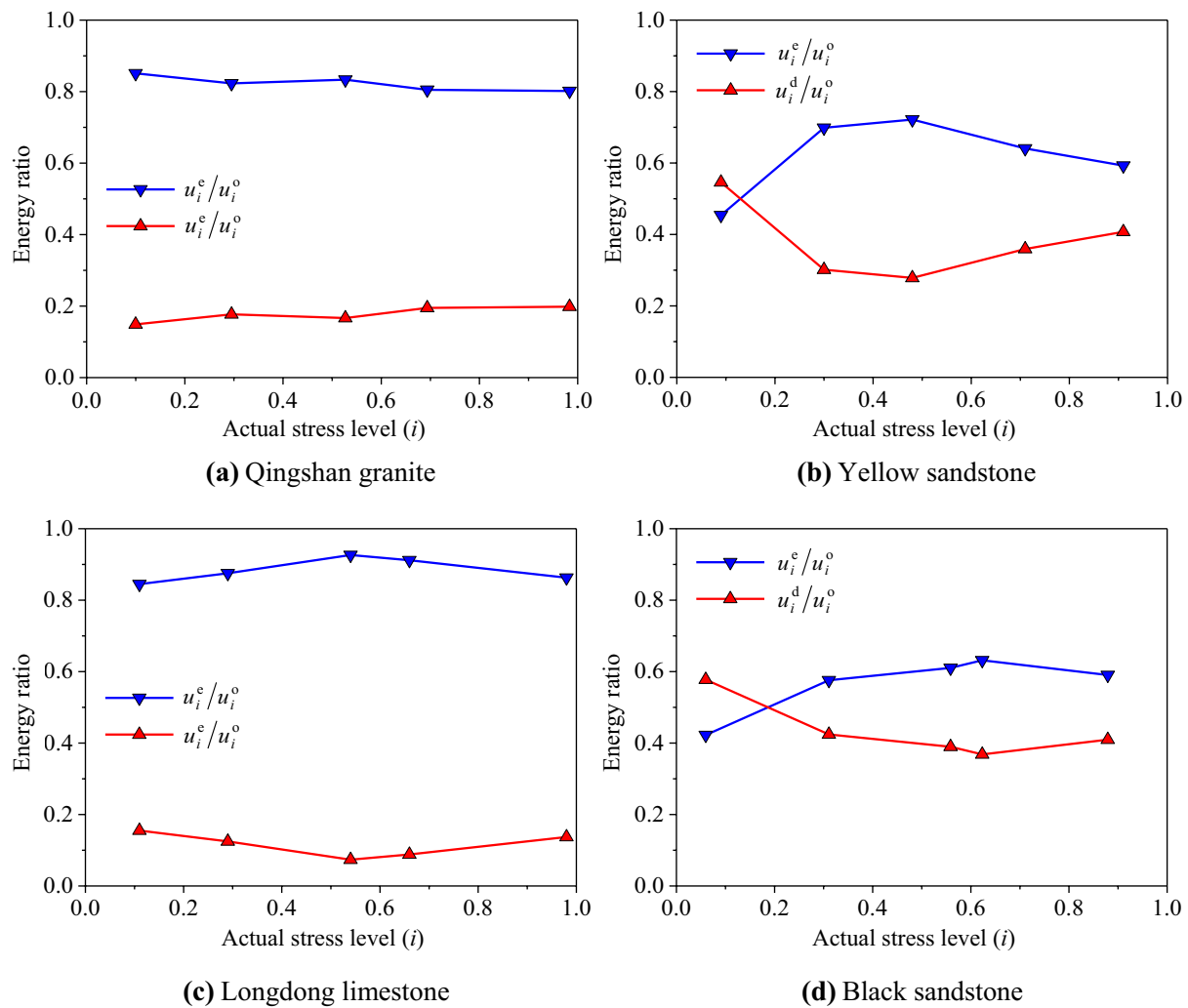


Fig. 9 Variation of the energy ratios of rock specimens with the actual stress level i

5 Discussion

The peak EED (u^e) plays an important role in investigating the mechanical characteristics of rocks. This term has attracted the attention of many researchers and has been used widely in many rock mechanic problems. Wang and Park (2001) reported that Kwasniewski et al. scaled the occurrence of shock and rockburst with u^e in their Scientific Report from 1994, and a criterion of elastic strain energy was presented to predict rockburst in Kwasniewski's private communication in 2000. Wang and Park (2001) applied this rockburst criterion to evaluate the rockburst proneness of rock in Linglong gold mine. Zhu et al. (2002) presented a new index of rockburst proneness using u^e . Xie et al. (2009) given the expression of u^e under the UC tests in establishing the overall failure criterion of the rock. Tarasov and Randolph (2011), Tarasov and Potvin (2013) discussed the superbrittleness of rocks and

universal criteria for rock brittleness considering u^e . Li et al. (2014) investigated the strain rate dependency of u^e under UC tests on coarse crystal marble. Huang and Li (2014) studied the conversion of u^e of marble in triaxial unloading tests. Munoz et al. (2016) proposed an energy-based brittleness index with u^e . Ai et al. (2016) gave two new brittleness indices including u^e . Cai (2016) and Miao et al. (2016) used u^e to estimate the rockburst proneness of six rocks in Sanshandao Gold Mine. Liu et al. (2017) introduced the peak elastic energy release rate using u^e .

The above research studies show that the accurate acquisition of u^e is very important and will directly affect the reliability and accuracy of analysis results. However, in actual UC tests, due to the discreteness and uncertainty of peak strength of rock specimens, it is impossible to unload in time enough at the peak strength of the specimen, and u^e cannot be obtained by calculating the area under the

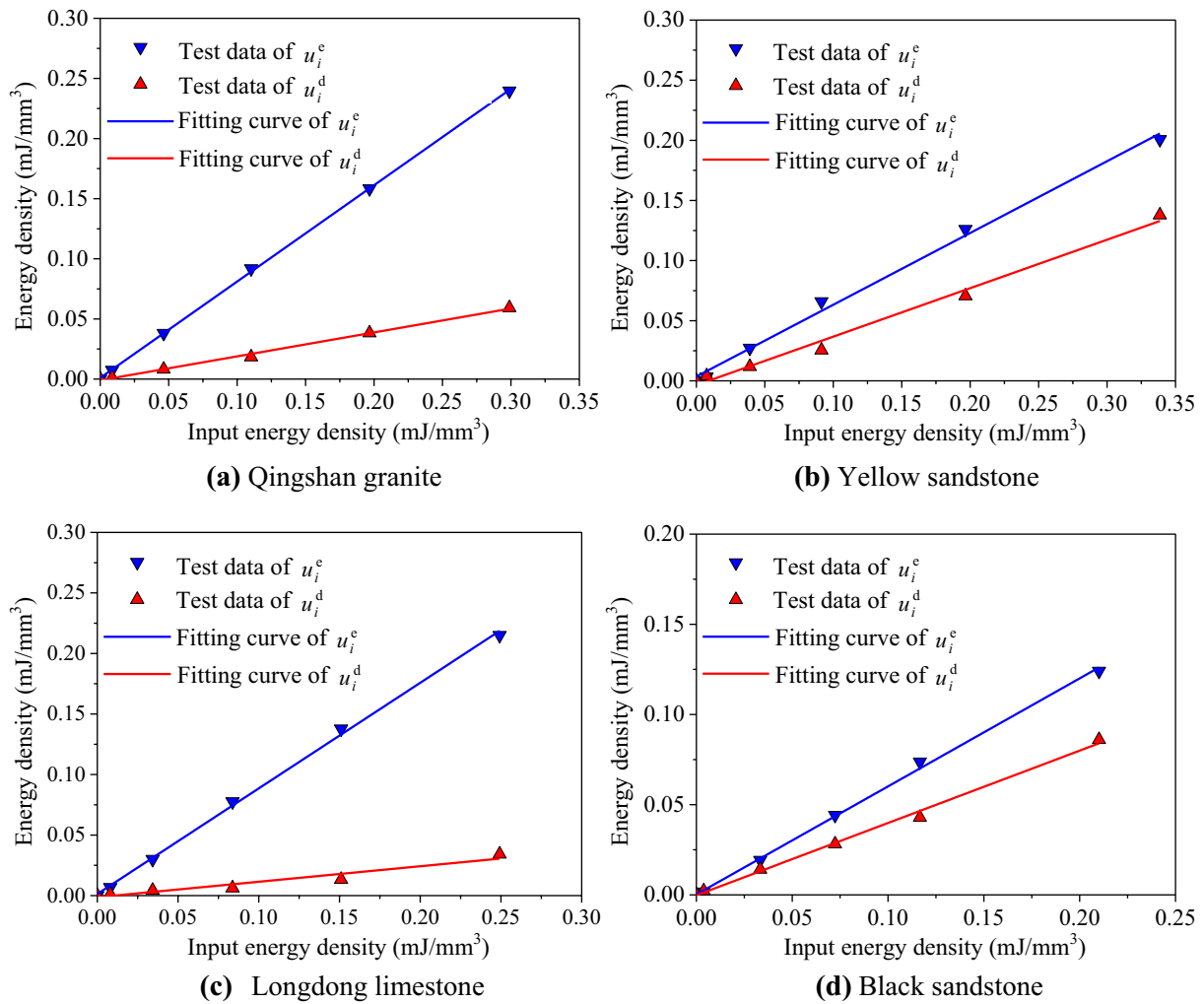


Fig. 10 Relationships between the EED and DED and IED

Table 5 Fitting functions and R^2 among u_i^o , u_i^e and u_i^d

Rock type	Fitting function for u_i^e and u_i^o	Fitting function for u_i^d and u_i^o	Fitting function for u_i^d and u_i^e
Qingshan granite	$u_i^e = 0.8010u_i^o + 0.0010$ ($R^2 = 0.9998$)	$u_i^d = 0.1990u_i^o - 0.0010$ ($R^2 = 0.9969$)	$u_i^d = 0.2481u_i^e - 0.0012$ ($R^2 = 0.9952$)
Yellow sandstone	$u_i^e = 0.5968u_i^o + 0.0036$ ($R^2 = 0.9953$)	$u_i^d = 0.4032u_i^o - 0.0036$ ($R^2 = 0.9899$)	$u_i^d = 0.6679u_i^e - 0.0055$ ($R^2 = 0.9717$)
Longdong limestone	$u_i^e = 0.8721u_i^o + 0.0014$ ($R^2 = 0.9986$)	$u_i^d = 0.1279u_i^o - 0.0014$ ($R^2 = 0.9377$)	$u_i^d = 0.1450u_i^e - 0.0014$ ($R^2 = 0.9132$)
Black sandstone	$u_i^e = 0.5989u_i^o + 0.0002$ ($R^2 = 0.9983$)	$u_i^d = 0.4011u_i^o - 0.0002$ ($R^2 = 0.9963$)	$u_i^d = 0.6668u_i^e - 0.0003$ ($R^2 = 0.9897$)

unloading curve. In most cases, the approximate expression of u^e is as follows (shown in Fig. 13):

$$u^e = \sigma_c^2 / 2E_u, \tag{9}$$

where σ_c is the peak strength of rock specimen in a UC test; E_u is regarded as the linear modulus of an ideal unloading curve at the peak strength point, and has different names in different literatures. When Eq. (9) was used to calculate the

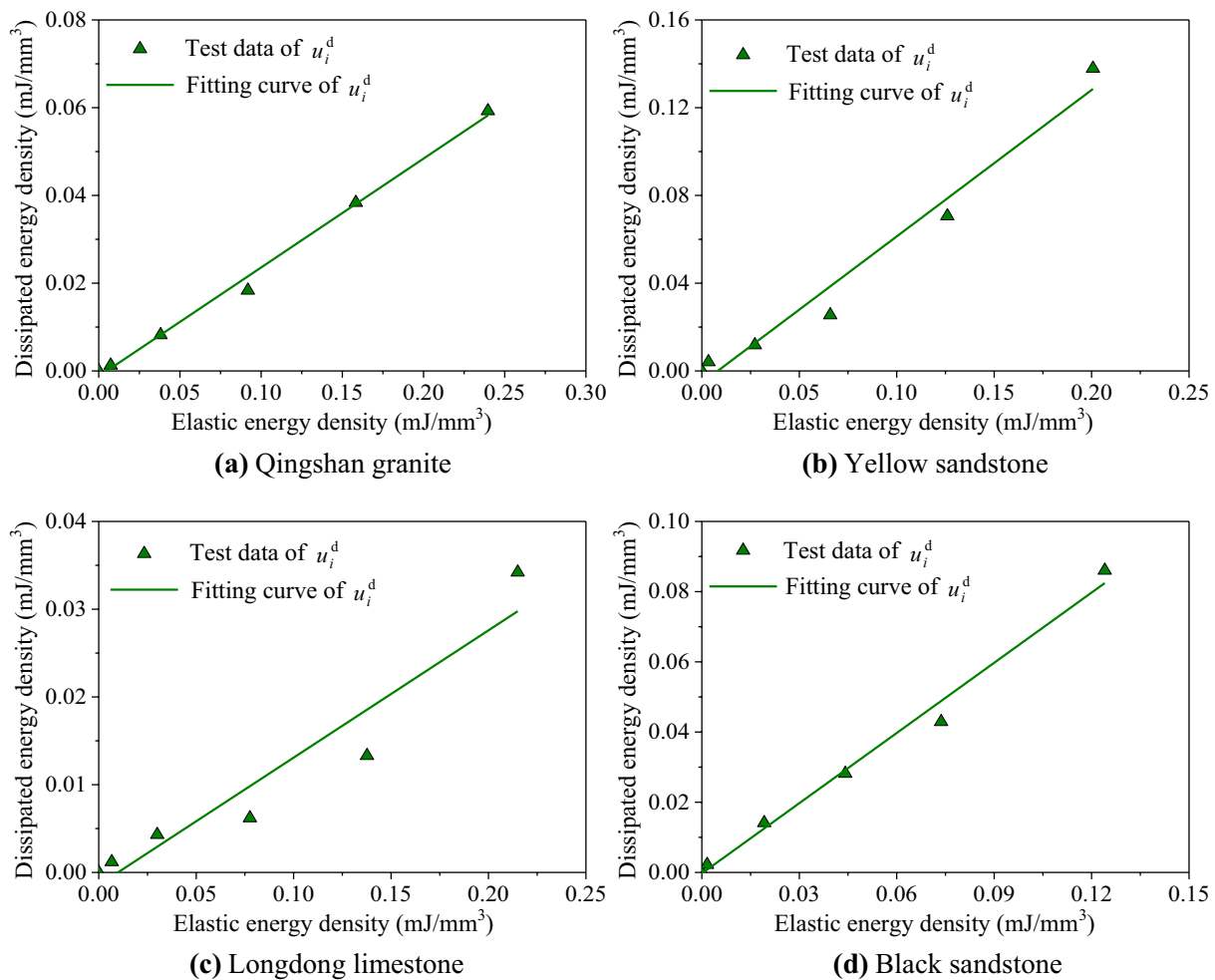


Fig. 11 Relationships between the dissipated and elastic energy density

value of u^e , two methods were often used to obtain E_u : (i) E_u is equal to the unloading tangential modulus E_s (Wang and Park, 2001, shown in Fig. 14a) (ii) E_u is equal to the Young's modulus of the loading curve E_l (Zhu et al. 2002 and Munoz et al. 2016, shown in Fig. 14b).

Two basic assumptions of Eq. (9) are: (i) the elastic modulus E_u is constant, that is, the unloading curve is a straight line; (ii) the unloading modulus E_u at the peak strength is equal to the unloading modulus E_s at a certain point before the peak strength. The aforementioned two basic assumptions are valid only for ideal linear elastic materials (shown in Fig. 15a). For natural rock materials, the unloading curve is not usually a straight line (shown in Fig. 15b). Since the unloading curve is not a straight line, E_u and E_s are not constants, and further E_u cannot be equal to E_s .

However, in our research in Sect. 4.4, there is a linear law between the EED, DED and IED. The u^o can be calculated using the graphical integration method in the stress–strain curve, and then u^e and u^d can be calculated easily using Eqs. (7) and (8). The presented method solves

the problem that E_u cannot be obtained scientifically and accurately.

After obtaining u_i^e and u_i^d , the variation of the ratio u_i^e / u_i^d (W_{et}^i) was also investigated. Equation (10) presents the formula of the traditional definition of W_{et}^i and the results of W_{et}^i are listed in Table 3.

$$W_{et}^i = \frac{u_i^e}{u_i^d}. \quad (10)$$

According to Eqs. (4) and (5), we give a new method for calculating dynamic W_{et}^d as follows:

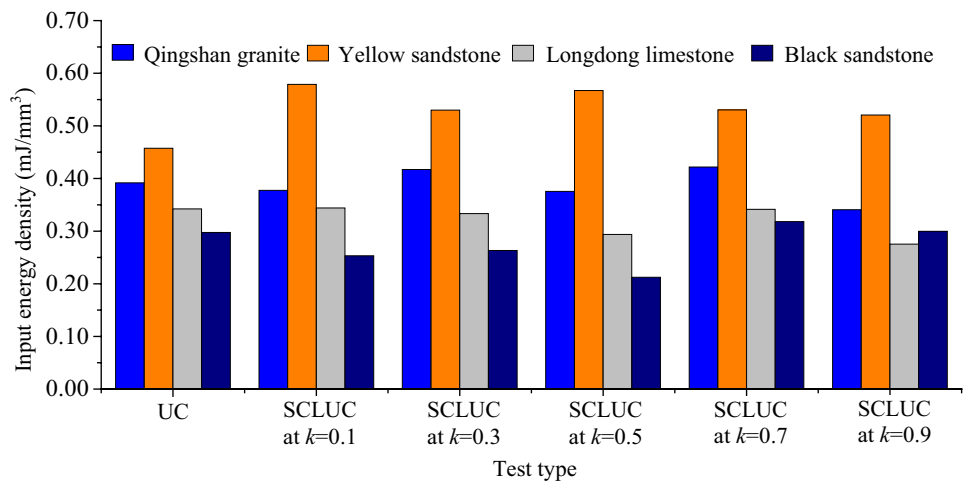
$$W_{et}^d = \frac{au_d^o + b}{(1-a)u_d^o - b}, \quad (11)$$

where u_d^o is the IED at any loading time before the peak compressive strength and W_{et}^d is the dynamic ratio of the EED to DED. The peak W_{et}^d is marked as W_{et}^p and can be expressed as follows:

Table 6 The u^o , u^e , u^d and W_{et}^p of rock specimens using the new method

Rock type	Specimen no.	u^o (mJ/mm ³)	u^e (mJ/mm ³)	u^d (mJ/mm ³)	u^e / u^d (W_{et}^p)	Average of u^e / u^d (W_{et}^p)
Qingshan granite	QM-1	0.3917	0.3148	0.0769	4.09	4.09
	QC-1	0.3776	0.3035	0.0741	4.10	
	QC-2	0.4172	0.3352	0.0820	4.09	
	QC-3	0.3755	0.3018	0.0737	4.09	
	QC-4	0.4218	0.3389	0.0829	4.09	
	QC-5	0.3406	0.2738	0.0668	4.10	
Yellow sandstone	YM-1	0.4575	0.2766	0.1809	1.53	1.52
	YC-1	0.5788	0.3490	0.2298	1.52	
	YC-2	0.5300	0.3199	0.2101	1.52	
	YC-3	0.5671	0.3420	0.2251	1.52	
	YC-4	0.5304	0.3201	0.2103	1.52	
	YC-5	0.5206	0.3143	0.2063	1.52	
Longdong limestone	LM-1	0.3422	0.2998	0.0424	7.07	7.10
	LC-1	0.3440	0.3014	0.0426	7.08	
	LC-2	0.3333	0.2921	0.0412	7.09	
	LC-3	0.2938	0.2576	0.0362	7.12	
	LC-4	0.3415	0.2992	0.0423	7.07	
	LC-5	0.2754	0.2416	0.0338	7.15	
Black sandstone	BM-1	0.2976	0.1784	0.1192	1.50	1.50
	BC-1	0.2531	0.1518	0.1013	1.50	
	BC-2	0.2633	0.1579	0.1054	1.50	
	BC-3	0.2125	0.1275	0.0850	1.50	
	BC-4	0.3181	0.1907	0.1274	1.50	
	BC-5	0.2998	0.1798	0.1200	1.50	

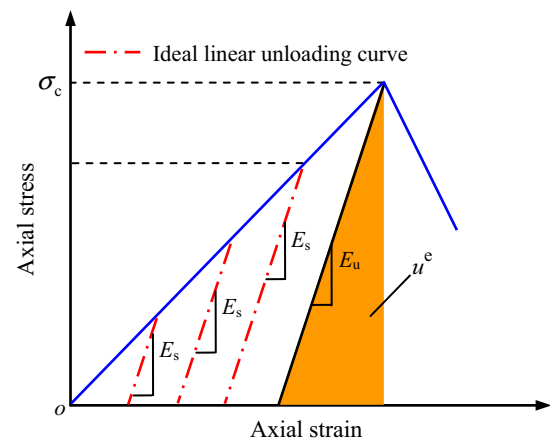
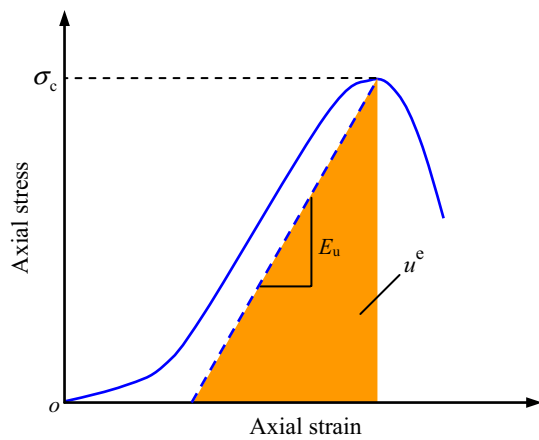
Fig. 12 The u^o of rock specimens in UC and SCLUC tests



$$W_{et}^p = \frac{au^o + b}{(1 - a)u^o - b} = \frac{u^e}{u^d} \tag{12}$$

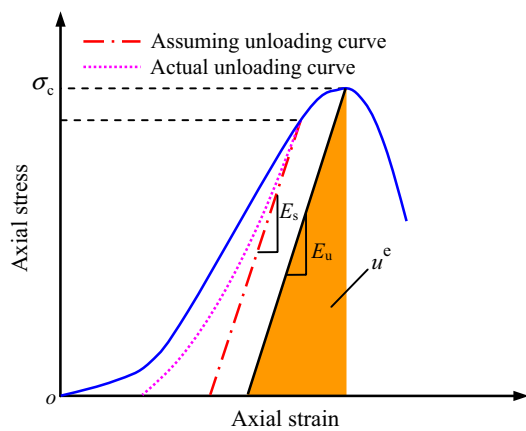
Figure 16 shows the variation trend of the ratio EED/DED from the traditional method and new method. With increasing IED, the volatility of W_{et}^i obtained by the traditional method is high, and W_{et}^i finally seems to converge,

which might require more experimental data for verification. However, the change curve of W_{et}^d tends to gradually converge with increasing IED increases. The values of W_{et}^p for the four rocks are given in Table 6. For comparison, the calculating results of u^e / u^d using two traditional methods are also shown in Tables 7 and 8. The results of the three methods are compared as shown in Fig. 17. It can be seen

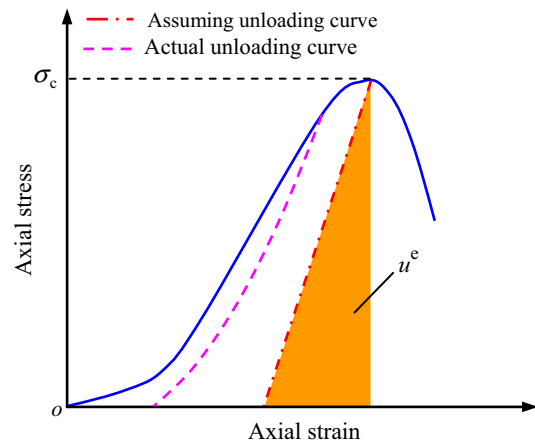


(a) Ideal linear elastic materials

Fig. 13 Schematic drawing of traditional calculation of u^e

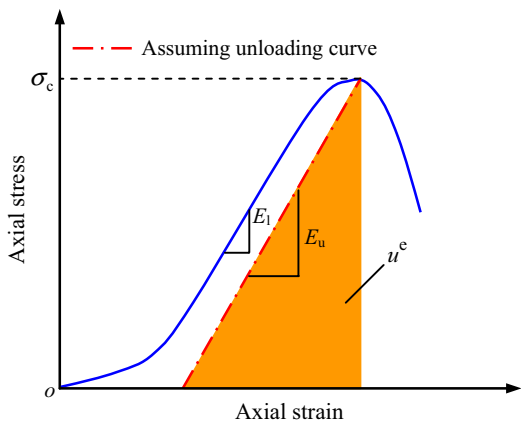


(a) $E_u = E_s$ by Wang and Park (2001)



(b) Natural rock materials

Fig. 15 Unloading curves of ideal linear elastic material and natural rock material



(b) $E_u = E_1$ by Zhu et al. (2002) and Munoz et al. (2016)

Fig. 14 Schematic drawing of calculation of E_u

that most of the u^e/u^d s using Method 1 are large than W_{et}^p s, while the u^e/u^d s using Method 2 are smaller than W_{et}^p s. The

reason for this characteristic is attributed to the hypothesis of two traditional methods. In addition, the randomness and dispersion of u^e/u^d s using two traditional methods are obvious. However, the values of W_{et}^p for every rock are very close to each other. The results indicate that W_{et}^p may be regarded as a constant that reflects the proportional of the elastic energy to the dissipation energy of rock material.

6 Conclusions

This paper investigated the energy evolution characteristics of four rock materials (Qingshan granite, Yellow sandstone, Longdong limestone and Black sandstone) under uniaxial compression using a series of SCLUC tests. Based on the test results, the following conclusions can be drawn:

- (1) In SCLUC tests, the secondary loading curves of rocks intersected the unloading curve at a stress slightly

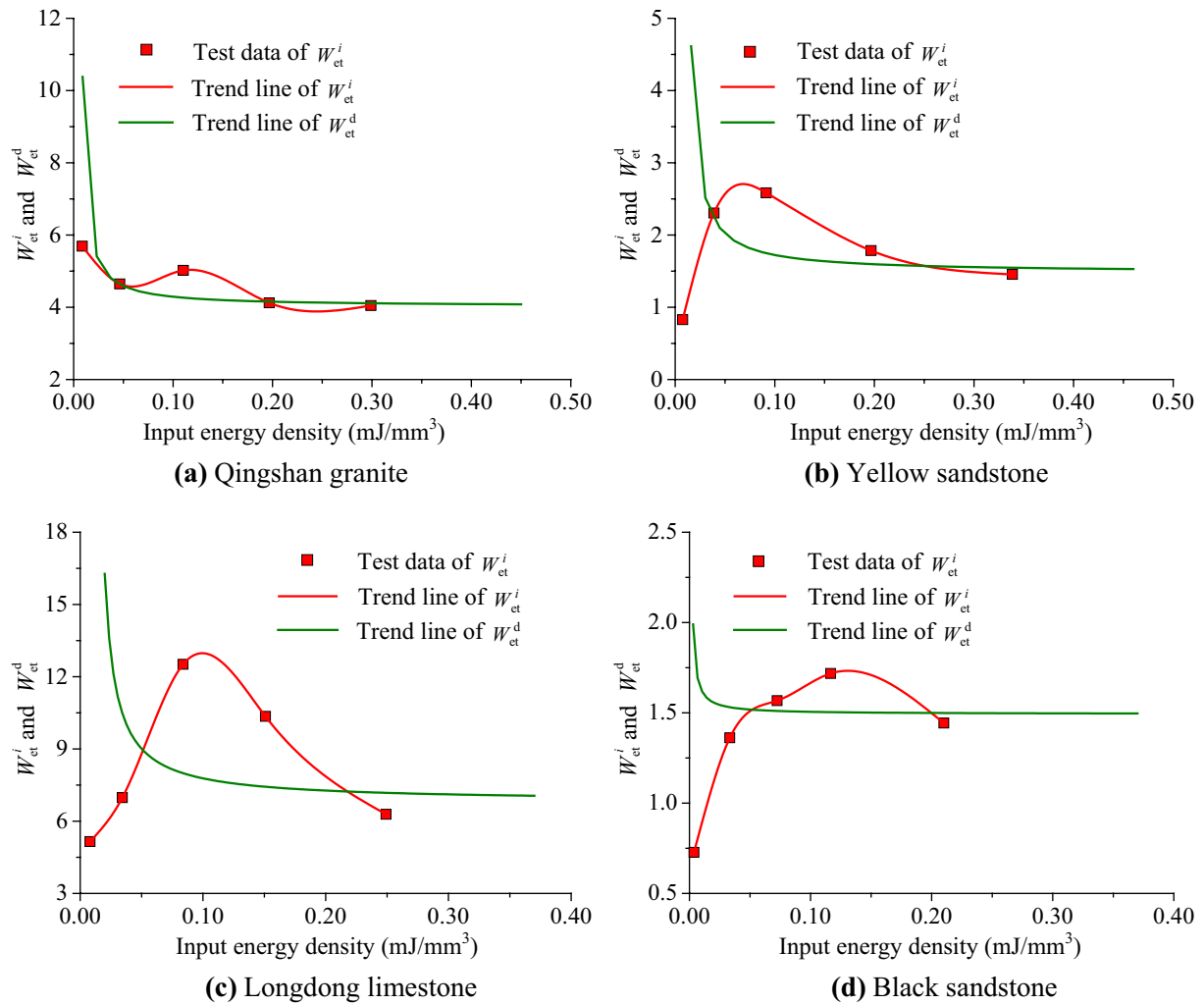


Fig. 16 Relationships between W_{et}^i and W_{et}^d and IED

smaller than unloading stress and continued to develop according to the development trend of the initial loading curve. The four rock materials possess memory, and the SCLUC process has minimal effect on the variation of the stress–strain curves. In addition, the failure modes of SCLUC are the same as those of UC.

- (2) The nonlinear characteristics of the energy evolution for four rock materials under different unloading stress levels were determined. Based on the analysis of the energy density parameters under different unloading stress levels, the IED, EED and DED all increase with

increasing stress as quadratic polynomial functions. The IED has the most rapid growth, following the EED, and finally the DED.

- (3) The linear relationships between EED and DED, and IED were obtained. The test results indicate that the EED and DED all increase linearly with increasing IED, and the linear energy storage or dissipation laws of rock materials were observed and confirmed. The EED and DED at any stress levels (including the peak compressive strength level) can be obtained using the linear energy storage or dissipation law above.

Table 7 The peak EED of rock specimens [the method of Zhu et al. (2002) and Munoz et al. (2016)]

Rock type	Specimen no.	$E_u (E_f)$ (GPa)	u^o (mJ/mm ³)	u^e (mJ/mm ³)	u^d (mJ/mm ³)	u^e / u^d	Average of u^e / u^d
Qingshan granite	QM-1	35.32	0.3917	0.3564	0.0353	10.10	6.82
	QC-1	36.57	0.3776	0.3300	0.0476	6.93	
	QC-2	36.76	0.4172	0.3728	0.0444	8.40	
	QC-3	36.15	0.3755	0.3306	0.0449	7.36	
	QC-4	37.67	0.4218	0.3489	0.0729	4.79	
	QC-5	39.33	0.3406	0.2620	0.0786	3.33	
Yellow sandstone	YM-1	14.73	0.4575	0.4057	0.0518	7.83	3.18
	YC-1	17.58	0.5788	0.4401	0.1387	3.17	
	YC-2	17.20	0.5300	0.3895	0.1405	2.77	
	YC-3	18.47	0.5671	0.4050	0.1621	2.50	
	YC-4	21.64	0.5304	0.3170	0.2134	1.49	
	YC-5	23.25	0.5206	0.2932	0.2274	1.29	
Longdong limestone	LM-1	44.61	0.3422	0.3236	0.0186	17.40	10.94
	LC-1	44.08	0.3440	0.2697	0.0743	3.63	
	LC-2	45.63	0.3333	0.3131	0.0202	15.50	
	LC-3	44.22	0.2938	0.2691	0.0247	10.89	
	LC-4	46.89	0.3415	0.3136	0.0279	11.24	
	LC-5	46.87	0.2754	0.2409	0.0345	6.98	
Black sandstone	BM-1	16.99	0.2976	0.2584	0.0392	6.59	4.33
	BC-1	16.40	0.2531	0.2086	0.0445	4.69	
	BC-2	16.22	0.2633	0.2238	0.0395	5.67	
	BC-3	17.83	0.2125	0.1696	0.0429	3.95	
	BC-4	18.77	0.3181	0.2402	0.0779	3.08	
	BC-5	19.60	0.2998	0.2004	0.0994	2.02	

Table 8 The peak EED of rock specimens [the method of Wang and Park (2001)]

Rock type	Specimen no.	$E_u(E_s)$ (GPa)	u^o (mJ/mm ³)	u^e (mJ/mm ³)	u^d (mJ/mm ³)	u^e / u^d
Qingshan granite	QC-5	43.09	0.3406	0.2391	0.1015	2.36
Yellow sandstone	YC-5	29.16	0.5206	0.2338	0.2868	0.82
Longdong limestone	LC-5	49.61	0.2754	0.2276	0.0478	4.76
Black sandstone	BC-5	25.57	0.2998	0.1536	0.1462	1.05

Where the unloading stress is near 90% peak stress of rock specimen

(4) The ratio EED/DED with the increase of IED was investigated. Due to the heterogeneity of natural rock materials, when the ratios EED/DED are directly calculated at different unloading stress levels using the experimental data, the ratio greatly fluctuates. In this research, we develop a new method to calculate the

ratio EED/DED. The results show that the change curve of the ratio tends to gradually converge as the IED increases. The ratio obtained at the peak compressive strength tends to be constant, which shows that there is a stable ratio EED/DED under UC of rock materials.

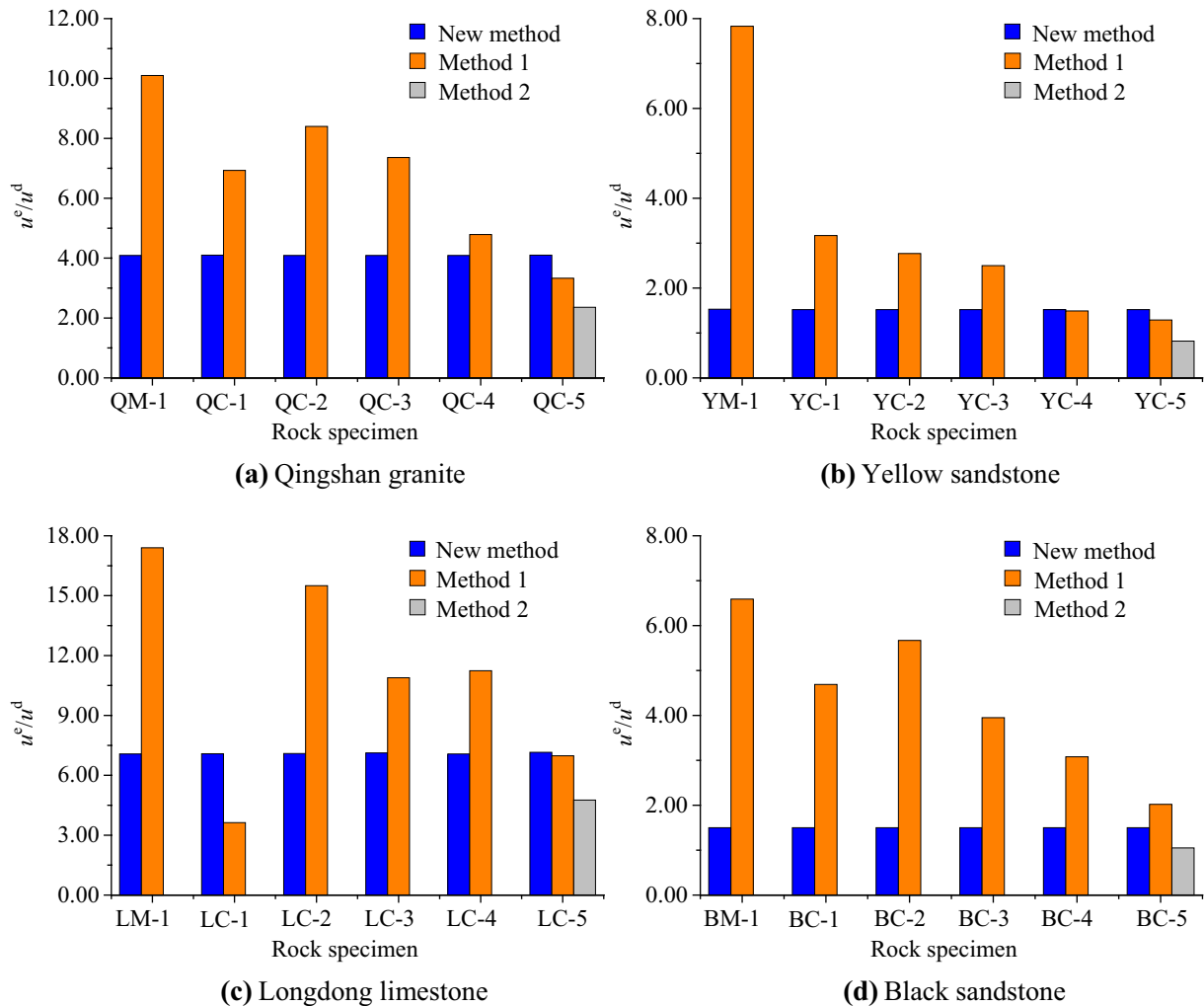


Fig. 17 The peak EED of rock specimens using three methods [Method 1: Zhu et al. (2002) and Munoz et al. (2016); Method 2: Wang and Park (2001)]

Acknowledgements This work was supported by the National Natural Science Foundation of China (Grant No. 41877272 and 41472269).

Compliance with ethical standards

Conflicts of interest The authors declare no conflict of interest.

References

- Ai C, Zhang J, Li YW, Zeng J, Yang XL, Wang JG (2016) Estimation criteria for rock brittleness based on energy analysis during the rupturing process. *Rock Mech Rock Eng* 49(12):4681–4698
- Brady BHG, Brown ET (2006) *Rock mechanics for underground mining*, 3rd edn. Springer, Dordrecht
- Cai MF (2016) Prediction and prevention of rockburst in metal mines: a case study of Sanshandao gold mine. *J Rock Mech Geotech Eng* 8(2):204–211
- Castanon-Jano L, Blanco-Fernandez E, Castro-Fresno D, Ballester-Munoz F (2017) Energy dissipating devices in falling rock protection barriers. *Rock Mech Rock Eng* 50(3):603–619
- Fairhurst CE, Hudson JA (1999) Draft ISRM suggested method for the complete stress–strain curve for intact rock in uniaxial compression. *Int J Rock Mech Min Sci* 36(3):281–289
- Gong FQ, Luo Y, Li XB, Si XF, Tao M (2018a) Experimental simulation investigation on rockburst induced by spalling failure in deep circular tunnels. *Tunn Undergr Space Technol* 81:413–427
- Gong FQ, Luo S, Li XB, Yan JY (2018b) Linear energy storage and dissipation rule of red sandstone materials during the tensile failure process. *Chin J Rock Mech Eng* 37(2):352–363
- Gong FQ, Luo S, Yan JY (2018c) Energy storage and dissipation evolution process and characteristics of marble in three tension-type failure tests. *Rock Mech Rock Eng* 51(11):3613–3624
- Gong FQ, Yan JY, Li XB, Luo S (2019) A peak-strength strain energy storage index for rock burst proneness of rock materials. *Int J Rock Mech Min Sci* 117:76–89
- Hua AZ, You MQ (2001) Rock failure due to energy release during unloading and application to underground rock burst control. *Tunn Undergr Space Technol* 16(3):241–246
- Huang D, Li YR (2014) Conversion of strain energy in triaxial unloading tests on marble. *Int J Rock Mech Min Sci* 66:160–168
- Jaeger JC, Cook NGW, Zimmerman RW (2007) *Fundamentals of Rock Mechanics*, 4th edn. Wiley, Oxford

- Jiang Q, Feng XT, Xiang TB, Su GS (2010) Rockburst characteristics and numerical simulation based on a new energy index: a case study of a tunnel at 2500 m depth. *Bull Eng Geol Environ* 69(3):381–388
- Kidybiński A (1981) Bursting liability indices of coal. *Int J Rock Mech Min Sci* 18(4):295–304
- Li SJ, Feng XT, Li ZH, Chen BR, Zhang CQ, Zhou H (2012) In situ monitoring of rockburst nucleation and evolution in the deeply buried tunnels of Jinping II hydropower station. *Eng Geol* 137–138:85–96
- Li YR, Huang D, Li XA (2014) Strain rate dependency of coarse crystal marble under uniaxial compression: strength, deformation and strain energy. *Rock Mech Rock Eng* 47(4):1153–1164
- Li JC, Rong LF, Li HB, Hong SN (2019) An SHPB test study on stress wave energy attenuation in jointed rock masses. *Rock Mech Rock Eng* 52:403–420
- Liu XF, Wang XR, Wang EY, Kong XG, Zhang C, Liu SJ, Zhao EL (2017) Effects of gas pressure on bursting liability of coal under uniaxial conditions. *J Nat Gas Sci Eng* 39:90–100
- Mcsaveney MJ, Davies TR (2009) Surface energy is not one of the energy losses in rock comminution. *Eng Geol* 109(1–2):109–113
- Meng QB, Zhang MW, Han LJ, Pu H, Nie TY (2016) Effects of acoustic emission and energy evolution of rock specimens under the uniaxial cyclic loading and unloading compression. *Rock Mech Rock Eng* 49(10):3873–3886
- Meng QB, Zhang MW, Han LJ, Pu H, Chen YL (2018) Acoustic emission characteristics of red sandstone specimens under uniaxial cyclic loading and unloading compression. *Rock Mech Rock Eng* 51(4):969–988
- Miao SJ, Cai MF, Guo QF, Huang ZJ (2016) Rock burst prediction based on in situ stress and energy accumulation theory. *Int J Rock Mech Min Sci* 83:86–94
- Munoz H, Taheri A, Chanda EK (2016) Rock drilling performance evaluation by an energy dissipation based rock brittleness index. *Rock Mech Rock Eng* 49(8):3343–3355
- Park JW, Park D, Ryu DW, Choi BH, Park ES (2014) Analysis on heat transfer and heat loss characteristics of rock cavern thermal energy storage. *Eng Geol* 181:142–156
- Peng RD, Ju Y, Wang JG, Xie HP, Gao F, Mao LT (2015) Energy dissipation and release during coal failure under conventional triaxial compression. *Rock Mech Rock Eng* 48(2):509–526
- Singh SP (1988) Burst energy release index. *Rock Mech Rock Eng* 21(2):149–155
- Song DZ, Wang EY, Liu J (2012) Relationship between EMR and dissipated energy of coal rock mass during cyclic loading process. *Saf Sci* 50(4):751–760
- Tarasov B, Potvin Y (2013) Universal criteria for rock brittleness estimation under triaxial compression. *Int J Rock Mech Min Sci* 59:57–69
- Tarasov BG, Randolph MF (2011) Superbrittleness of rocks and earthquake activity. *Int J Rock Mech Min Sci* 48(6):888–898
- Torabi A, Zarifi Z (2014) Energy release rate of propagating deformation bands and their hosted cracks. *Int J Rock Mech Min Sci* 67:184–190
- Tsoutrelies CE, Exadaktylos GE (1993) Effect of rock discontinuities on certain rock strength and fracture energy parameters under uniaxial compression. *Geotech Geol Eng* 11(2):81–105
- Wang JA, Park HD (2001) Comprehensive prediction of rockburst based on analysis of strain energy in rocks. *Tunn Undergr Space Technol* 16(1):49–57
- Wang P, Xu JY, Fang XY, Wang PX (2017) Energy dissipation and damage evolution analyses for the dynamic compression failure process of red-sandstone after freeze-thaw cycles. *Eng Geol* 221:104–113
- Wasantha PLP, Ranjith PG, Shao SS (2014) Energy monitoring and analysis during deformation of bedded-sandstone: use of acoustic emission. *Ultrasonics* 54(1):217–226
- Xie HP, Ju Y, Li LY (2005) Criteria for strength and structural failure of rocks based on energy dissipation and energy release principles. *Chin J Rock Mech Eng* 24(17):3003–3010
- Xie HP, Li LY, Peng RD, Ju Y (2009) Energy analysis and criteria for structural failure of rocks. *J Rock Mech Geotech Eng* 1(1):11–20
- Xu YH, Cai M (2018) Influence of strain energy released from a test machine on rock failure process. *Can Geotech J* 55(6):777–791
- Yang YM, Ju Y, Li FX, Gao F, Sun HF (2016) The fractal characteristics and energy mechanism of crack propagation in tight reservoir sandstone subjected to triaxial stresses. *J Nat Gas Sci Eng* 32:415–422
- Zhang ZZ, Gao F (2015) Experimental investigation on the energy evolution of dry and water-saturated red sandstones. *Int J Min Sci Technol* 25(3):383–388
- Zhang MW, Meng QB, Liu SD (2017) Energy evolution characteristics and distribution laws of rock materials under triaxial cyclic loading and unloading compression. *Adv Mater Sci Eng* 2017:1–16
- Zhu FC, Pan CL, Guo R (2002) A new rock burst proneness index-effective impact energy index. *J Min Safety Eng* 19(3):83–84

Publisher's Note Springer Nature remains neutral with regard to jurisdictional claims in published maps and institutional affiliations.